ELSEVIER

Biophysical Chemistry 128 (2007) 245–252

Biophysical Chemistry

http://www.elsevier.com/locate/biophyschem

Integration host factor alters LacI-induced DNA looping

Chiara Zurla [d], Tomas Samuely [b], Giovanni Bertoni [a], Francesco Valle [c], Giovanni Dietler [c], Laura Finzi [d], David D. Dunlap [e,*]

[a] *Department of Biomolecular Sciences and Biotechnologies, University of Milan, Italy*
[b] *Institut für Physik, Universität Basel, Switzerland*
[c] *Laboratoire de Physique de la Matière Vivante, Ecole Polytechnique Fédérale de Lausanne, Switzerland*
[d] *Department of Physics, Emory University, Atlanta, GA, USA*
[e] *Department of Cell Biology, Emory University, Atlanta, GA, USA*

Received 16 March 2007; received in revised form 20 April 2007; accepted 20 April 2007
Available online 3 May 2007

Abstract

The integration host factor protein of *Escherichia coli*, which sharply bends DNA at specific sites and non-specifically compacts the bacterial genome, can also alter looping of DNA in an artificial system based on the lactose repressor protein of *E. coli*. In single molecule experiments, we show that both specific bending and non-specific compaction alter LacI-mediated looping of DNA. Our results highlight the subtle regulatory roles that proteins, which confer structure upon DNA, might have in controlling DNA transcription and other processes in which the conformation of DNA determines the binding and activity of processive enzymes.

Keywords: Integration host factor; Lactose repressor; DNA looping; Tethered particle motion; Scanning or atomic force microscopy

1. Introduction

Active DNA management by the cell is instrumental for genome propagation and expression. Some of the factors that influence DNA topology are the flexibility of the DNA and the binding of proteins that induce torsion, bending or looping. Often, there is interplay between supercoiling, bending and looping of the double helix in order to achieve a particular architecture [1]. Genome structure is usually maintained by dedicated proteins, which organize DNA into the highly ordered structures found, for example, in eukaryotic chromatin. Although, bacteria lack histone-mediated chromatin structures, the bacterial genome is also well organized in a compact structure called the nucleoid [2,3]. A set of some 10–20 DNA-binding proteins maintains the nucleoid structure in *Escherichia coli* and are referred to as nucleoid-associated proteins or simply "nucleoid proteins" and in some cases "histone-like proteins" for their functional resemblance to eukaryotic histones [4,5]. The major *E. coli* proteins involved in compaction and organization of the nucleoid are several small and very abundant proteins including the heat unstable (HU), histone-like nucleoid structuring (H-NS), integration host factor (IHF) and factor of inversion simulation (FIS) proteins.

The association of genomic DNA with nucleoid proteins determines its overall conformation by inducing wrapping, packaging, bending and coiling. General nucleoid structuring and its consequences for genome dynamics are believed to result from non-specific DNA binding. However, some nucleoid proteins bind DNA at preferential sites and thus alter DNA architecture in a specific manner [6]. These architectural changes can strongly influence genome dynamics, namely replication, transcription, recombination and repair.

IHF is a well-characterized nucleoid protein involved in site-specific recombination, DNA replication and transcription [6]. In most of these processes, it facilitates the formation of nucleoprotein structures by inducing conformational changes in the DNA. IHF binds tightly (K_d=2–20 nM) to defined target sites with consensus WATCARXXXXTTR (W: A or T; R: A or G; X: A, T, C or G) generally resulting in a sharp DNA bend of ~160°.

* Corresponding author. Cell Biology Department, Emory University School of Medicine, 615 Michael Street, Atlanta, GA 30322, USA. Tel.: +1 404 727 7729; fax: +1 404 727 6256.
E-mail address: ddunlap@emory.edu (D.D. Dunlap).

0301-4622/$ - see front matter © 2007 Elsevier B.V. All rights reserved.
doi:10.1016/j.bpc.2007.04.012

This specific DNA binding and bending activity of IHF was shown to play a key architectural role in several cellular processes such as replication initiation at *oriC*, site-specific recombination, phage packaging and regulation of transcription initiation.

IHF can either enhance or inhibit transcription, depending on the relative position of the binding sites of regulators, IHF, and RNA polymerase (RNAP) [7–10]. For instance, IHF acts as an architectural element in the regulation of the transcription of several σ^{54}-dependent promoters [10–13]. In such systems, IHF bends the DNA upon binding to a specific site located between the promoter and enhancer sites and facilitates looping the DNA to bring the σ^{54}-activator pre-bound at the enhancer toward σ^{54}-RNAP assembled in a closed complex. At some promoters of this kind, IHF also stimulates closed complex formation by σ^{54}-RNAP at the promoter DNA by bringing together C-terminal domains of the RNAP α subunits and A+T-rich promoter sequences, the UP elements, located upstream of the core promoter region [14].

IHF also binds more weakly to random DNA sequences (K_d= 20–30 μM). This weaker, non-specific DNA binding activity is nonetheless considered to be physiologically relevant, given that the IHF concentration in the cell ranges from 10 to 100 μM, with an increase at the onset of the stationary growth phase [9]. IHF binding to low-affinity random sites induces compaction of DNA with or without consensus sequences and the extent of compaction increases with IHF concentrations up to ~500 nM [15]. IHF-mediated DNA compaction is supposed to play a pivotal role in modulating nucleoid structure. However, the effect of IHF-mediated compaction on other cellular processes is poorly understood.

Thus, we investigated how specific, sharp bending or non-specific compaction of DNA by IHF affected DNA looping induced by the lactose repressor (LacI), a well-characterized transcriptional regulatory protein [16]. LacI is an ideal model system for the present study, since it has been well-characterized both with single molecules techniques, such as tethered particle motion (TPM) and fluorescence resonance energy transfer [17,18], and traditional assays. Extensive analysis has shown that LacI-mediated repression is influenced by LacI specific binding site sequences, separation and phasing [19–21]. DNA bending by IHF has also been detected in single molecule experiments in which it reduced the extension of single DNA molecules by 8 nm [22]. The present results indicate that concentration-dependent regimes of IHF binding in conjunction with characteristics of particular DNA sequences can either favor or obstruct LacI-mediated looping.

2. Experimental

2.1. DNA templates and proteins

The DNA templates L0 (732 bp), L1 (891 bp), L2 (1073 bp), L3 (1199), L4 (1288 bp) and L6 (1495 bp), were provided by Opher Gileadi (Quantomix Ltd, Rehovot, Israel). A plasmid from the Müller-Hill laboratory, pO_{id}-O1, which contains the two high-affinity *lac* operators O_{id} (5′-TGTGAGCGCTCACA-3′) [23,24] and O1 (5′-AATTGTGAGCGGATAACAATT-3′) 70 bp apart, served as a template for PCR amplification of the DNA fragment L0. The PCR reaction was performed using two primers: (5′-GCCACCTCTGACTTAAGCGTCG-3′) with an AflII restriction site and (5′-TTGAGGGGACGTCGACAGTA-TC-3′) with a SalI restriction site. The plasmid pO_{id}-O1 also served to produce a series of plasmids in which the *lac* operators are separated by varying distances by the insertion of "stuffer" DNA fragments ranging from 100 bp to 700 bp and containing the IHF-specific binding site H1 (5′-TATGCAGT-CACTATGAATCAACTACTTAGATGGT-3′). The engineered plasmids were then used as templates to amplify L1, L2, L3, L4 and L6 fragments, respectively, by PCR with the same primers used for L0. DNA fragments for the TPM experiments were then labelled at the ends by first cleaving with SalI and filling in the 3′-recessed ends with biotinylated dUTP (Roche Diagnostics GmbH, Mannheim, Germany) and unlabelled dATP, dGTP and dCTP. After inactivation of the DNA polymerase (Klenow, Fermentas UAB, Vilnius, Lithuania) and purification through a spin column (Biorad P30, Bio-Rad, Hercules, California), the DNA was cleaved with AflII and overhangs were filled with dig-UTP (Roche Diagnostics GmbH, Mannheim, Germany) and unlabelled dATP, dGTP and dCTP. Finally, the DNA was separated from the free nucleotides with a PCR purification kit (Qiagen GmbH, Hilden, Germany).

IHF was supplied by S. Goodman (University of California, Los Angeles, California) and LacI was supplied by K.S. Matthews (Rice University, Houston, Texas).

2.2. Preparation of the flow chamber for tethered particle motion

The flow chambers for TPM measurements were similar to those described by Finzi and Dunlap [25]. A flow chamber was incubated for 30 min with 20 μg/ml anti-digoxigenin (Sigma) in PBS. After washing the flow chamber with 800 μl of LacI buffer (10 mM Tris–HCl pH 7.4, 200 mM KCl, 5% DMSO, 0.1 mM EDTA, 0.2 mM DTT and 0.1 mg/ml α-casein) biotin- and digoxigenin-labelled DNA was introduced and incubated for 1 h before washing out unbound DNA with 800 μl LacI buffer. An excess of streptavidin-coated beads (430 nm in diameter) in LacI buffer lacking DTT and DMSO was then introduced and incubated for 30 min. Unattached beads were then flushed from the chamber with LacI buffer. Experiments with LacI (2.5–5 nM) were carried out in LacI buffer and the indicated concentrations of IHF.

2.3. Tethered particle motion (TPM) measurement

Video-enhanced, differential interference contrast micrographs of the tethered beads were recorded with a CCD camera (JAI A60, Copenhagen, Denmark) at 25 frames/s on a SuperVHS recorder. Images were digitized with a PCI-1409 frame grabber (National Instruments, Austin, Texas, USA) and analyzed using custom software to determine the x and y coordinates of the bead versus time. The mean of the x and y coordinates establishes the anchor point of the DNA on the glass. The Brownian motion of the bead was then calculated as $R = \sqrt{(x-\overline{x})^2+(y-\overline{y})^2}$ and smoothed with a 100-point, moving average. In discriminating

between the extended and the looped conformations of all DNA fragments, values less than or equal to 123.7 nm, equivalent to the mean end-to-end distance of L0 plus two standard deviations, $R_0+2\sigma_0$, were assumed to correspond to the looped conformation of the other DNA fragments.

2.4. Atomic force microscopy (AFM)

The DNA fragments for AFM were diluted in a buffer containing 10 mM TRIS pH 7.6, 200 mM KCl, 10 mM EDTA, 20 mM DTT to a final DNA concentration of 0.5 μg/ml. A small droplet (10 μl) of sample was then placed onto the substrate surface and left to adsorb for approximately 10 min at room temperature; the sample was then rinsed with nanopure (Ultra High Quality) water (USF Elga, High Wycombe, England) and blown dry with clean air.

For the measurements done in the presence of the proteins, the DNA fragments were incubated with LacI (0.2 μg/ml) and IHF (0.025 μg/ml) at room temperature for 10 min before deposition onto the substrate surface.

The surface used for DNA imaging in this work was AP-mica. This surface was produced by exposing freshly cleaved mica to the vapor of 3-Aminopropyltriethoxysilane (APTES) for 2 h in an Argon atmosphere following a published protocol [26]. Images were recorded using a Nanoscope IIIa (Veeco Inc, Woodbury, NY, USA) operated in tapping mode in air. The ultrasharp non-contact silicon cantilevers (NT-MDT Co., Zelenograd, Moskow, Russia) used had a nominal tip radius of <10 nm and were driven at oscillation frequencies in the range of 150 to 300 kHz. During imaging, the mica surface was scanned at a rate of one line per second. Images were simply flattened using the Nanoscope III software without further processing.

The DNA molecules were analyzed using "Ellipse" software (Slovak Academy of Science of Kosice) [27] to trace each molecule and to accurately measure the contour length. The digitization procedure is based on the well-known "Snake" algorithm.

3. Results

The DNA fragments used have two LacI binding sites (operators): O1, the highest affinity wild-type site, and O_{id}, a synthetic binding site whose affinity for LacI is 6 times higher. The IHF-specific binding site, derived from the H1 sequence within the lambda *attP* region [28], was inserted between the two operators 97–114 bp from the O_{id} sequence. The distance between the IHF binding site and O1 increases from 113 to 718 bp in steps of about 100–200 bp in fragments L1 to L6 (Fig. 1).

3.1. IHF-mediated DNA bending and compaction

First, using the tethered particle motion (TPM) technique [18], we measured the architectural effect of IHF on DNA fragments L2, L3, L4 and L6 which contain a specific IHF binding site. Fig. 2a shows the amplitude of Brownian motion of DNA-tethered beads, which depends on the average extension of the DNA, as a function of IHF concentration. At low protein concentrations, IHF was expected to bind preferentially

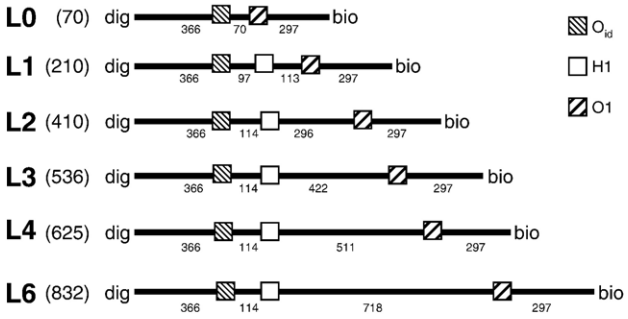

Fig. 1. The DNA fragments for AFM (L1) and TPM (L2, L3, L4 and L6): *lac* operators (hatched boxes) and the H1 binding site (empty boxes) as well as distances (bp) between the centers of binding sites are indicated. The spacing between the O_{id} and O1 sites is indicated in parentheses. H1 and O1 are differently spaced in the six fragments. L0, L2, L3, L4 and L6 were labelled at one end with digoxigenin and at the other end with biotin.

to the specific binding sites within the fragments and induce very little DNA compaction. However, we expected the amplitude of Brownian motion of the tethered beads to decrease due to bending of the DNA at the IHF binding site. In fact, this amplitude decreased upon addition of 1 nM IHF for all fragments, and three out of four differently sized tethers decreased by 10 nm (Fig. 2a). Instead the Brownian motion of beads attached to the same DNA in the presence of competing oligonucleotides or devoid of an IHF binding site did not decrease (Supplementary information). At higher concentrations, IHF was expected to also distribute non-specifically along the DNA fragments and induce a certain degree of DNA compaction depending on the particular DNA sequence, which affects i) the overall affinity for the protein and ii) the malleability of the double helix [15,29]. At higher IHF concentrations, Brownian motion of tethered beads decreased by ~20–26% for L4 or L6, and ~10% for L2 or L3 (at 100 nM IHF). The decreased Brownian motion was consistent with the DNA compaction reported in similar experiments by Ali et al. [15]. IHF-induced compaction at 125 nM IHF was also observed using atomic force microscopy (AFM) of the L1 fragment (Fig. 2b).

3.2. Effects of IHF-mediated bending on LacI-induced DNA looping

The DNA fragments represented in Fig. 1 were expected to be looped by simultaneous binding of tetrameric LacI to two high-affinity LacI binding sites, O_{id} and O1, placed on either side of an IHF binding site. In order to characterize the influence of IHF interactions with DNA on LacI-mediated DNA looping, we performed TPM measurements in the presence of LacI alone or in combination with IHF, both at a low concentration of 1 nM, and higher concentrations of 50 or 100 nM (see below).

For L2, L3, L4 and L6, the LacI-mediated DNA loop formation and breakdown produced a bimodal frequency distribution of the amplitude of Brownian motion as determined by TPM (Fig. 3; L3 data not shown). Before addition of LacI, the percentage of time spent by DNA molecules in the looped

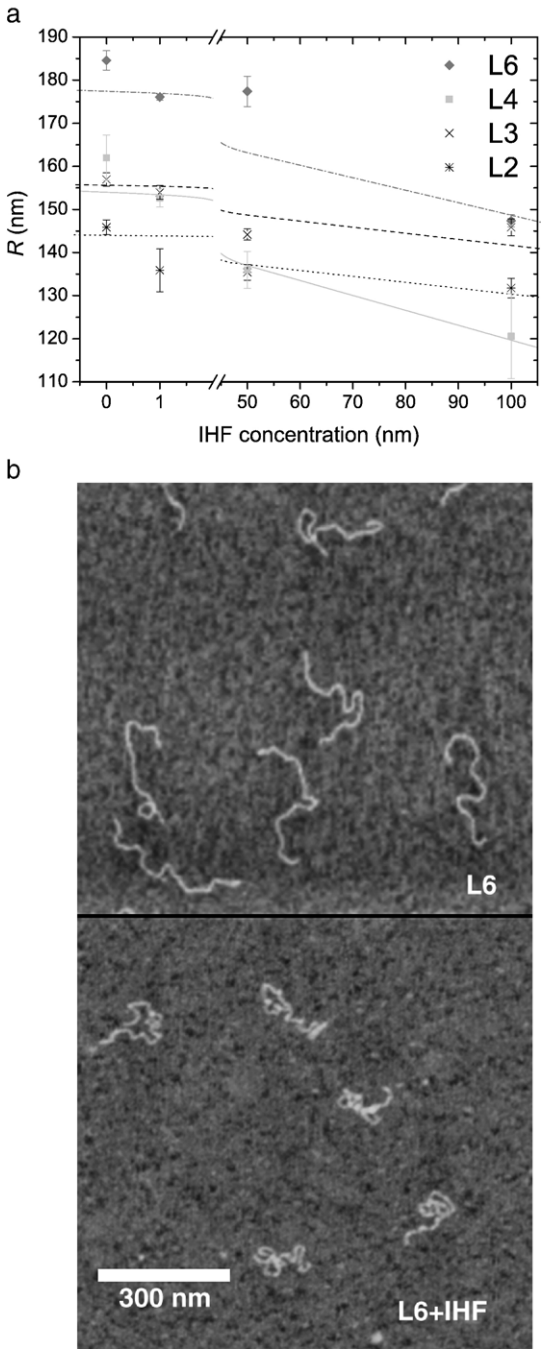

Fig. 2. a) Effect of IHF concentration on the Brownian motion of the bead *(R)* for beads tethered by DNA fragments L2, L3, L4 and L6. *R* decreases in L2 (black), L3 (blue), L4 (red) and L6 (green), as the concentration of IHF increases from 1 nM to 100 nM. Error bars represent the standard error and the lines are linear fits. b) AFM visualization of the DNA fragment L6 alone (upper) and in the presence of 125 nM IHF (lower).

conformation was negligible (Table 1). In the presence of LacI, the DNA molecules spent more time in the looped conformations even with separations between the binding sites as large as those of L4 and L6. Although the efficiency of loop formation did not correlate well with the size of the loop, these results showed that LacI binding to the high-affinity operators efficiently looped all the DNA fragments.

To assess the effects of IHF bending on LacI-mediated looping, we repeated these experiments in the presence of 1 nM IHF. Fig. 3a is an example of the frequency distributions of the amplitude of Brownian motion of L4-tethered beads in the presence of LacI with and without 1 nM IHF. Such data was used to determine the effect of specific IHF binding on the

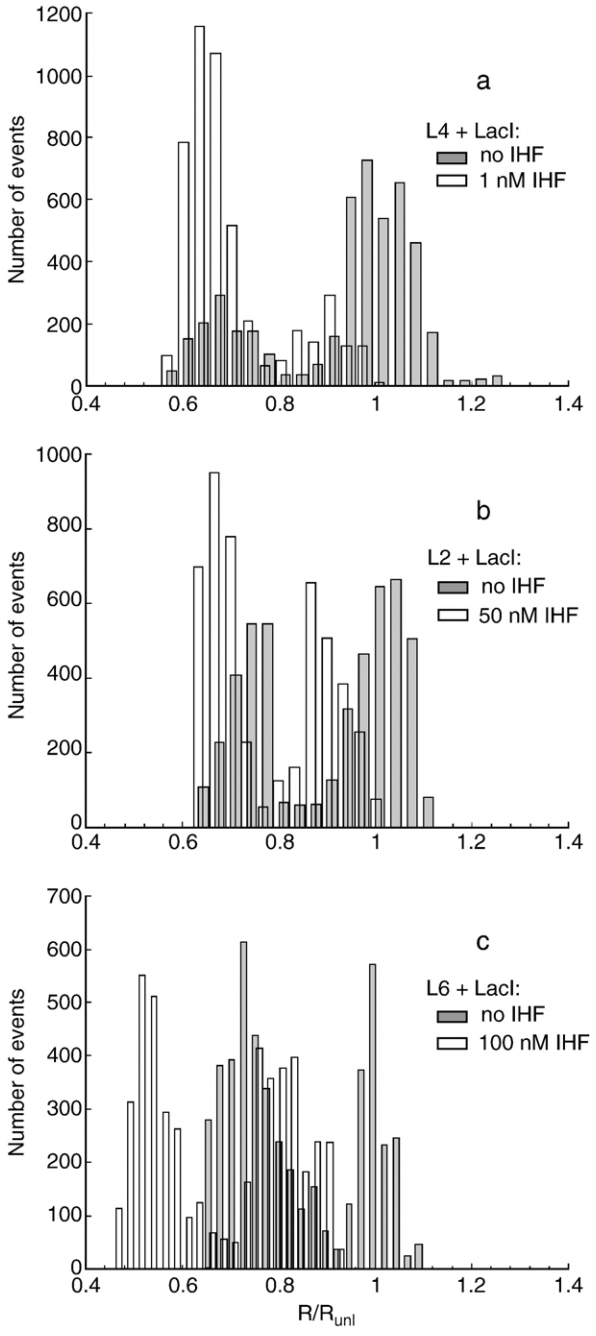

Fig. 3. Effect of IHF on LacI-mediated DNA looping. Representative distributions of normalized Brownian motion (R / $R_{unlooped}$) measured using TPM are shown for LacI and DNA fragment: (a) L4 with 1 nM IHF, (b) L2 with 50 nM IHF and (c) L6 with 100 nM IHF. LacI produced bimodal frequency distributions with (red) or without IHF (blue). The expected values of normalized Brownian motion for looped L2, L4, and L6 fragments are 0.82, 0.78 and 0.75 respectively. These values were estimated using the base pair intervals listed in Figure 1, a bead radius of 215 nm, and a persistence length of 43 nm [33].

ability of LacI to mediate DNA looping in fragments L2, L4 and L6 (Fig. 5). IHF promoted looping in the case of L4, and hindered it in the cases of L2 and L6.

Since the L1 loop was so short, it was difficult to detect using TPM. Therefore the effect of 1 nM IHF on LacI-induced DNA looping of this fragment was evaluated using AFM [26]. AFM images of L1 alone, in the presence of LacI and in the presence of both LacI and IHF 1nM were analysed by measuring the "apparent" contour length of each molecule bypassing, in the tracing process, the small, LacI-induced nodes along the molecule (see Supplementary information). This strategy was adopted due to the difficulty of accurately tracing the path of the DNA associated with protein in these nodes. We verified that, in our experimental conditions, the contour lengths of DNA fragments deposited on mica were not altered by 1 nM IHF (data not shown). The histograms in Fig. 4 show the distributions of the contour lengths measured for L1, L1 with LacI, and L1 with LacI and IHF. The addition of LacI shifts a fraction of the contour length distribution toward shorter values of contour length (Table 1). The addition of both LacI and IHF further shifts the frequency distribution toward the looped DNA conformation (Table 1). These distributions are statistically different as shown by Kolmogorov–Smirnov tests, and the effect of IHF is specific, since corresponding distributions for a fragment without an IHF binding site did not shift (Supplementary information).

Assuming that the molecules in the AFM images are derived from an equilibrium between looped and unlooped conformations, a Boltzman expression was used to estimate the energy difference between the unlooped and looped configurations,

$$\frac{N_{\text{looped}}}{N_{\text{total}}} = e^{\frac{-\Delta E}{k_B T}} \quad (1)$$

Furthermore, to quantify how IHF enhances looping, the change in the free energy of LacI-induced looping with and without IHF, $\Delta E_{\text{IHF}} = \Delta E_{\text{IHF+LacI}} - \Delta E_{\text{LacI}}$, was calculated. Considering Boltzman's distributions on equal samplings of molecules, this expression becomes

$$\Delta E_{\text{IHF}} = k_B T \ln\left(\frac{N_{\text{looped}_{\text{LacI}}}}{N_{\text{looped}_{\text{IHF+LacI}}}}\right) \quad (2)$$

In measurements at room temperature, $\Delta E_{\text{IHF}} = k_B T \ln(196/341) = -0.6\ k_B T$.

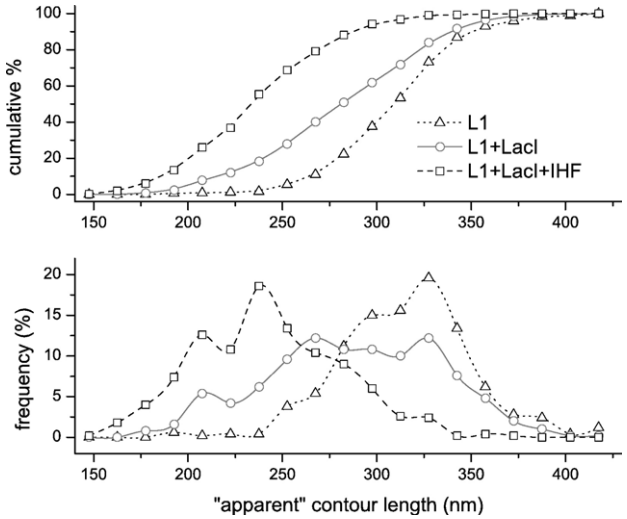

Fig. 4. IHF (1 nM) promotes LacI-induced looping in L1. The "apparent" contour length of the DNA fragment L1 was measured using AFM. Cumulative (upper) and normalized (lower) histograms for L1 (red triangles), L1+LacI (black circles), and L1+ LacI + IHF (green rhombi). Estimates based on the base pair lengths in Figure 1 multiplied by 0.335 nm/bp indicate that looped and unlooped molecules should be 222 and 292 nm in length respectively. All but the L1+LacI+IHF distribution were determined to be non-normal distributions by Shapiro-Wilk testing using Origin software (OriginLab Corp., Northampton, MA). Kolmogorov-Smirnov, non-parametric tests [35] indicate significant differences between these non-normal distributions: L1 vs. L1+LacI, maximum cumulative difference (D)=0.2920 and $P<0.001$; L1+LacI vs. L1+LacI+IHF, D=0.4220 and $P<0.001$.

Table 1
Percent occupancy of the looped conformation for the DNA fragments L1, L2, L3 L4 and L6, the equilibrium constant of the looping reaction (k_{eq}), and the additional energy contributed by IHF to LacI-mediated DNA looping

LacI	IHF (nM)	% looped	keq	ΔEIHF (kT)
L1				
–	–	–	–	
+	–	39	0.64	−0.6±0.072
+	1	68	2.12	
+	50	–	–	
+	100	–	–	
L2				
–	–	3	0.03	
+	–	43	0.75	0.3±0.26
+	1	33	0.49	
+	50	48	0.92	
+	100	84	5.25	
L3				
–	–	1	0.01	
+	–	23	0.30	
+	1	–	–	
+	50	–	–	
+	100	75	3.00	
L4				
–	–	1	0.01	
+	–	50	1.00	−0.3±0.16
+	1	70	2.30	
+	50	43	0.75	
+	100	33	0.49	
L6				
–	–	0	0.00	
+	–	60	1.50	1.4±0.32
+	1	15	0.18	
+	50	39	0.64	
+	100	34	0.52	

The standard deviations associated with the energy estimates were estimated by assuming that the percentages of looped molecules derive from binomial distributions. With sample sizes of 400 for AFM and tens of thousands for TPM, the probability of looping is the percentage, $\frac{\bar{x}}{N}$, of looping and the standard deviation was calculated as s.d. $= \sqrt{Npq} = \sqrt{Np(1-p)}$. The standard deviations of the energy contributions by IHF were calculated as $dE = kT(\Delta x/x + \Delta y/y)$ using partial derivatives.

A similar analysis was performed with the data from TPM experiments, and the effect of IHF on looping in each experimental condition is summarized in Table 1. 1 nM IHF stabilizes loop formation by $-0.3\ k_BT$ in L4 and destabilizes it to the same extent in L2. 1 nM IHF hindered looping in L6 to a greater extent, with $\Delta E_{IHF} = 1.4\ k_BT$. The most dramatic changes were observed for the shortest and the longest DNA fragments respectively, but in opposite directions.

3.3. Effects of IHF-mediated compaction on LacI-induced DNA looping

In order to investigate the effect of DNA compaction induced by IHF on loop formation, TPM experiments were performed with fragments L2, L4 and L6 in the presence of LacI and 50 nM IHF. Fig. 3b shows that, with or without 50 nM IHF, the frequency distributions of the amplitude of Brownian motion of L2-tethered beads were bimodal. However, the peaks corresponding to the looped and the unlooped conformations in the presence of IHF were slightly shifted towards smaller values compared to those without IHF. Such shifts were likely due to IHF-induced DNA compaction and not alternative loop closures as discussed by Semsey et al. [30].

The equilibrium constants calculated for looping of the three DNA fragments, calculated from percentages of time spent in the looped and unlooped conformations, are plotted in Fig. 5. Compared to LacI alone, LacI plus 50 nM IHF slightly enhanced loop formation in the case of L2 while it hindered the formation of loops in L4 and L6.

Similar experiments were performed using 100 nM IHF. Fig. 3c shows the frequency distributions of the amplitude of Brownian motion measured for L6-tethered beads in the presence of LacI with and without 100 nM IHF. In the presence of IHF, the DNA fragments significantly shortened with respect to the length observed with LacI alone but Brownian motion remained bimodally distributed. The plot of equilibrium constants for looping (Fig. 5) shows that 50 or 100 nM IHF produced similar effects on the various DNA fragments with respect to LacI alone; high IHF concentrations favored loop formation in L2 and hindered it in L4 and L6. 100 nM IHF also promoted looping in the intermediately sized fragment, L3. Interestingly, both L2 and L3 compacted to a lesser degree in the presence of high concentrations of IHF (Fig. 2) than L4 and L6. Thus the enhancement of looping by IHF was inversely correlated with the degree of compaction promoted by IHF.

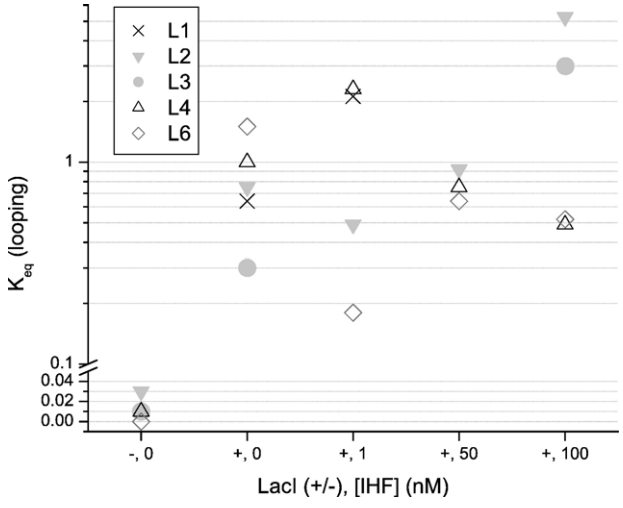

Fig. 5. Equilibrium constants for looping were calculated from the numbers of looped and unlooped molecules (AFM) or time percentages of looped and unlooped states (TPM). Without LacI there is essentially no looping. Low concentrations of IHF unpredictably changed looping in different fragments. Instead, higher concentrations enhanced looping in shorter fragments (L1–L3) and hindered looping in longer fragments (L4 and L6).

4. Discussion

TPM experiments are surprisingly sensitive and single bends in DNA molecules have been observed for a catalytically inactive transposase [31]. In the present experiments, 1 nM IHF also noticeably shortened DNA tethers (Fig. 2). Increasing the concentration of IHF decreased the average extension of DNA as a result of a non-specific binding of the protein. This indicated DNA compaction, since stiffening of the DNA tether such as that seen with non-specific binding by the HU protein [32] would tend to increase the average extension and Brownian motion [33]. The extent of the compaction we observed in the DNA fragments L4 and L6 in the presence of an excess of IHF is similar to the 25–30% compaction observed by Ali Jaffar and collaborators both in TPM and magnetic tweezing assays [15]. We also found that the DNA fragments L2 and L3, the shortest fragments we analyzed by TPM, were less compacted by IHF. The binding affinity of IHF to DNA is thought to vary over a large range of values, from the nanomolar affinity of canonical sites, to 10^{-7}–10^{-6} M, or even higher values, depending on differences in local DNA flexibility [15]. Therefore relatively more flexible fragments might have bound high amounts of IHF. However a "BEND IT" analysis [34] revealed only single, very stiff segments found in the longer fragments (Supplementary information), which might be expected to decrease IHF binding and attenuate DNA compaction.

IHF also significantly influenced LacI-mediated looping. In control conditions (LacI without IHF), the distance between the operators and the stiffness of the DNA fragment included in the loop seemed to affect looping efficiency. Indeed, looping was favored in the L4 and L6 fragments with respect to L2, which is less flexible. Adding 1 nM IHF substantially enhanced looping in L1 and L4 but mildly or significantly inhibited looping of L2 and L6 respectively. In L6, the position of the IHF binding site is quite asymmetric with respect to the two lac operators which might have inhibited loop closure. In fact previous evidence indicates that the bend induced upon IHF binding to a specific site may inhibit the activation of transcription if the site is asymmetrically located between the promoter and the activator [8].

Although seemingly large differences in the time (for TPM data) or number (for AFM data) percentages of the looped conformation were observed, IHF, which does not directly interact with LacI, only weakly changed the stability of the looped configuration with respect to experiments in which only LacI was present. For example, AFM analysis showed that 1 nM IHF only stabilized loop formation in L1 by $-0.6\ k_BT$

(Table 1). Similar analysis for the three fragments observed using TPM showed that IHF shifted the looping equilibrium by no more than a factor of 4 ($=e^{1.4}$) in a direction dependent on the specific fragment. Although basing the threshold for looping on uncompacted DNA might have led to underestimations of the degree of looping in IHF-compacted DNA, it is also possible that other elements of protein–DNA and protein–protein interactions dominate long range, transcriptional regulation paradigms that involve both looping and bending proteins [1].

5. Conclusions

The data revealed that the specific distances between sites along the DNA molecule profoundly influenced the alteration of DNA looping by IHF binding and bending. Interestingly, the most dramatic effects were visible in L1, where H1 is centered between O_{id} and O1, and in L6, where H1 is over 700 bp away from O1. Therefore, in the presence of IHF, the relative distances, and, for short DNA segments, the phasing of the protein binding sites become critical parameters. As a result, whether an IHF-specific bend favors or hinders looping may depend on loop length and bend placement.

Instead the effect of IHF-induced DNA compaction upon LacI-mediated looping inversely correlated with loop length. High concentrations of IHF enhanced shorter L2 and L3 loops and attenuated longer L4 and L6 loops (Fig. 5). However the L2 and L3 fragments were also compacted less by IHF than L4 and L6 (Fig. 2a) perhaps indicating a threshold of compaction beyond which LacI-induced looping is attenuated. Further experiments will be necessary to test these hypotheses. The present results are consistent with the idea that compaction by IHF attenuates LacI-looping in the case of distant operators and enhances it in the case of those nearby. This might be a general way in which chromatin-like compaction limits protein-induced looping to proximal binding sites in the genome.

Acknowledgments

We are grateful to Opher Gileadi for providing initial constructs and primers, Carlo Manzo for assistance with data analysis, and to Steve Goodman (University of Southern California, Los Angeles, CA) and Kathleen Matthews (Rice University, Houston, Texas) for proteins. This work was supported by the Italian Ministry of Instruction, Universities and Research (FIRB 2001, D.D. and L.F.; COFIN 2002, L.F.) and the Human Frontier Science Program (L.F.).

Appendix A. Supplementary data

Supplementary data associated with this article can be found, in the online version, at doi:10.1016/j.bpc.2007.04.012.

References

[1] G. Lia, D. Bensimon, V. Croquette, J.F. Allemand, D. Dunlap, D.E. Lewis, S. Adhya, L. Finzi, Supercoiling and denaturation in Gal repressor/heat unstable nucleoid protein (HU)-mediated DNA looping, 100 (2003) 11373–11377.
[2] P.E. Pettijohn, The nucleoid, (1996) 158–166.
[3] L.J. Wu, Structure and segregation of the bacterial nucleoid, 14 (2004) 126–132.
[4] T.A. Azam, S. Hiraga, A. Ishihama, Two types of localization of the DNA-binding proteins within the *Escherichia coli* nucleoid, 5 (2000) 613–626.
[5] T.A. Azam, A. Ishihama, Twelve species of the nucleoid-associated protein from *Escherichia coli*. Sequence recognition specificity and DNA binding affinity, 274 (1999) 33105–33113.
[6] K.K. Swinger, P.A. Rice, IHF and HU: flexible architects of bent DNA, 14 (2004) 28–35.
[7] D.F. Browning, J.A. Cole, S.J. Busby, Transcription activation by remodelling of a nucleoprotein assembly: the role of NarL at the FNR-dependent *Escherichia coli* nir promoter, 53 (2004) 203–215.
[8] N. Goosen, P. van de Putte, The regulation of transcription initiation by integration host factor, 16 (1995) 1–7.
[9] S.M. McLeod, R.C. Johnson, Control of transcription by nucleoid proteins, 4 (2001) 152–159.
[10] H. Xu, T.R. Hoover, Transcriptional regulation at a distance in bacteria, 4 (2001) 138–144.
[11] M. Carmona, V. de Lorenzo, G. Bertoni, Recruitment of RNA polymerase is a rate-limiting step for the activation of the sigma(54) promoter Pu of *Pseudomonas putida*, 274 (1999) 33790–33794.
[12] V. de Lorenzo, M. Herrero, M. Metzke, K.N. Timmis, An upstream XylR- and IHF-induced nucleoprotein complex regulates the sigma 54-dependent Pu promoter of TOL plasmid, 10 (1991) 1159–1167.
[13] T.R. Hoover, E. Santero, S. Porter, S. Kustu, The integration host factor stimulates interaction of RNA polymerase with NIFA, the transcriptional activator for nitrogen fixation operons, 63 (1990) 11–22.
[14] R. Macchi, L. Montesissa, K. Murakami, A. Ishihama, V. De Lorenzo, G. Bertoni, Recruitment of sigma 54-RNA polymerase to the Pu promoter of *Pseudomonas putida* through integration host factor-mediated positioning switch of alpha subunit carboxyl-terminal domain on an UP-like element, 278 (2003) 27695–27702.
[15] B.M. Ali, R. Amit, I. Braslavsky, A.B. Oppenheim, O. Gileadi, J. Stavans, Compaction of single DNA molecules induced by binding of integration host factor (IHF), 98 (2001) 10658–10663.
[16] C.E. Bell, M. Lewis, The Lac repressor: a second generation of structural and functional studies, 11 (2001) 19–25.
[17] L.M. Edelman, R. Cheong, J.D. Kahn, Fluorescence resonance energy transfer over approximately 130 basepairs in hyperstable lac repressor-DNA loops, 84 (2003) 1131–1145.
[18] L. Finzi, J. Gelles, Measurement of lactose repressor-mediated loop formation and breakdown in single DNA molecules, 267 (1995) 378–380.
[19] W.T. Hsieh, P.A. Whitson, K.S. Matthews, R.D. Wells, Influence of sequence and distance between two operators on interaction with the lac repressor, 262 (1987) 14583–14591.
[20] J. Muller, S. Oehler, B. Muller-Hill, Repression of lac promoter as a function of distance, phase and quality of an auxiliary lac operator, 257 (1996) 21–29.
[21] S. Oehler, M. Amouyal, P. Kolkhof, B. von Wilcken-Bergmann, B. Muller-Hill, Quality and position of the three lac operators of *E. coli* define efficiency of repression, 13 (1994) 3348–3355.
[22] S. Dixit, M. Singh-Zocchi, J. Hanne, G. Zocchi, Mechanics of binding of a single integration-host-factor protein to DNA, 94 (2005) 118101.
[23] J.R. Sadler, H. Sasmor, J.L. Betz, A perfectly symmetric lac operator binds the lac repressor very tightly, 80 (1983) 6785–6789.
[24] A. Simons, D. Tils, B. von Wilcken-Bergmann, B. Muller-Hill, Possible ideal lac operator: *Escherichia coli* lac operator-like sequences from eukaryotic genomes lack the central G X C pair, 81 (1984) 1624–1628.
[25] L. Finzi, D. Dunlap, Single-molecule studies of DNA architectural changes induced by regulatory proteins, 370 (2003) 369–378.
[26] Y.L. Lyubchenko, A.A. Gall, L.S. Shlyakhtenko, R.E. Harrington, B.L. Jacobs, P.I. Oden, S.M. Lindsay, Atomic force microscopy imaging of double stranded DNA and RNA, 10 (1992) 589–606.
[27] J. Marek, E. Demjenova, Z. Tomori, J. Janacek, I. Zolotova, F. Valle, M. Favre, G. Dietler, Interactive measurement and characterization of DNA molecules by analysis of AFM images, 63 (2005) 87–93.
[28] J.A. Goodrich, M.L. Schwartz, W.R. McClure, Searching for and predicting the activity of sites for DNA binding proteins: compilation and analysis of the

binding sites for *Escherichia coli* integration host factor (IHF), 18 (1990) 4993–5000.
[29] R. Jauregui, C. Abreu-Goodger, G. Moreno-Hagelsieb, J. Collado-Vides, E. Merino, Conservation of DNA curvature signals in regulatory regions of prokaryotic genes, 31 (2003) 6770–6777.
[30] S. Semsey, M.Y. Tolstorukov, K. Virnik, V.B. Zhurkin, S. Adhya, DNA trajectory in the Gal repressosome, 18 (2004) 1898–1907.
[31] N. Pouget, C. Turlan, N. Destainville, L. Salome, M. Chandler, IS911 transpososome assembly as analysed by tethered particle motion, 34 (2006) 4313–4323.
[32] J. van Noort, S. Verbrugge, N. Goosen, C. Dekker, R.T. Dame, Dual architectural roles of HU: formation of flexible hinges and rigid filaments, 101 (2004) 6969–6974.
[33] P.C. Nelson, C. Zurla, D. Brogioli, J.F. Beausang, L. Finzi, D. Dunlap, Tethered particle motion as a diagnostic of DNA tether length, 110 (2006) 17260–17267.
[34] K.Vlahovicek, L. Kajan, S. Pongor, DNA analysis servers: plot.it, bend.it, model.it and IS, 31 (2003) 3686–3687.
[35] T.W. Kirkman, Statistics to Use (1996), http://www.physics.csbsju.edu/stats/, accessed April 16, 2007.; MatLab software (Mathworks, Natick, Massachussets, USA).